Chloritoid-kyanite schists from the Veporic unit, Western Charpathians, Slovakia : implications for Alpine (Cretaceous) metamorphism

Autor(en): **Lupták, Branislav / Janák, Marian / Plašienka, Dušan**

Objekttyp: **Article**

Zeitschrift: **Schweizerische mineralogische und petrographische Mitteilungen = Bulletin suisse de minéralogie et pétrographie**

Band (Jahr): **80 (2000)**

Heft 2

PDF erstellt am: **26.09.2024**

Persistenter Link: https://doi.org/10.5169/seals-60962

SCHWEIZ. MINERAL. PETROGR. MITT. 80, 213–223, 2000

Chloritoid-kyanite schists from the Veporic unit, Western Carpathians, Slovakia: implications for Alpine (Cretaceous) metamorphism

by *Branislav Lupták*[1], *Marian Janák*[2], *Dušan Plašienka*[2], *Suzanne Th. Schmidt*[3] and *Martin Frey*[3]

Abstract

Alpine metamorphism related to Cretaceous orogeny has been investigated in the south-eastern part of the Veporic unit in the Western Carpathians. Permian pelitic schists contain the mineral assemblage chloritoid + kyanite + chlorite + quartz + white mica (muscovite–phengite–paragonite) ± ilmenite ± rutile. Deformational microtextures show that regional metamorphic foliation was transposed into the shear planes due to (top-to-the E) deformation, related to extension and exhumation. Chloritoid is mostly zoned, with increasing $X_{Mg} = Mg/(Mg + Fe^{2+})$ from core to rim as a consequence of prograde Fe^{2+}-Mg cation exchange between chloritoid and coexisting chlorite. A reverse pattern is interpreted as retrograde zoning of chloritoid porphyroblasts. Estimated peak metamorphic conditions obtained from thermobarometric calculations yield the temperature of 530–560 °C and pressure of 6–8 kbar. Estimated P-T conditions in the chloritoid-kyanite schists from the Permo-Triassic cover in the Veporic unit suggest substantial crustal thickening in the Western Carpathians during Cretaceous continental collision after the closure of the Meliata ocean. The development of S–C fabric is consistent with post-burial orogen-parallel extension and unroofing of the Veporic core complex.

Keywords: chloritoid-kyanite schists, P-T conditions, Alpine metamorphism, Veporic unit, Western Carpathians.

Introduction

The Central Western Carpathians, located between the Meliatic and Penninic-Vahic oceanic sutures, originated by shortening and stacking of a continental domain which was related to Europe during the Late Paleozoic and Triassic, and to Apulia during the Cretaceous and Tertiary. The pre-Tertiary complexes of the Central Western Carpathians are composed of six principal Slovakocarpathian north-verging superunits: the Tatric, Veporic and Gemeric thick-skinned basement/cover sheets and the Fatric, Hronic and Silicic detachment cover nappe systems (for a review see e.g. BIELY, 1989; PUTIŠ, 1991; TOMEK, 1993; PLAŠIENKA et al., 1997). All these units originated during the Cretaceous collisional shortening and stacking of the lower plate following the closure of the Meliatic ocean by the Late Jurassic (PLAŠIENKA, 1997) and they may be well correlated with the Austroalpine units of the Alps. Metamorphism related to Cretaceous, so called "Eoalpine" events in the Austroalpine units of the Eastern Alps, reached amphibolite facies and in several places even eclogite facies (e.g. FRANK, 1987; THÖNI and JAGOUTZ, 1992; FREY et al., 1999; HOINKES et al., 1999).

Metamorphic consequences of Cretaceous orogeny in the Western Carpathians are relatively poorly understood, mainly because of a complex polymetamorphic history of the pre-Alpine basement. Consequently, the intensity and extent of

[1] Department of Mineralogy and Petrology, Comenius University, Mlynská dolina G, 842 15 Bratislava, Slovak Republic. <bluptak@fns.uniba.sk>
[2] Geological Institute, Slovak Academy of Sciences, Dúbravská 9, 842 26 Bratislava, Slovak Republic.
[3] Mineralogisch-Petrographisches Institut, Universität Basel, Bernoullistrasse 30, CH-4056 Basel, Switzerland.

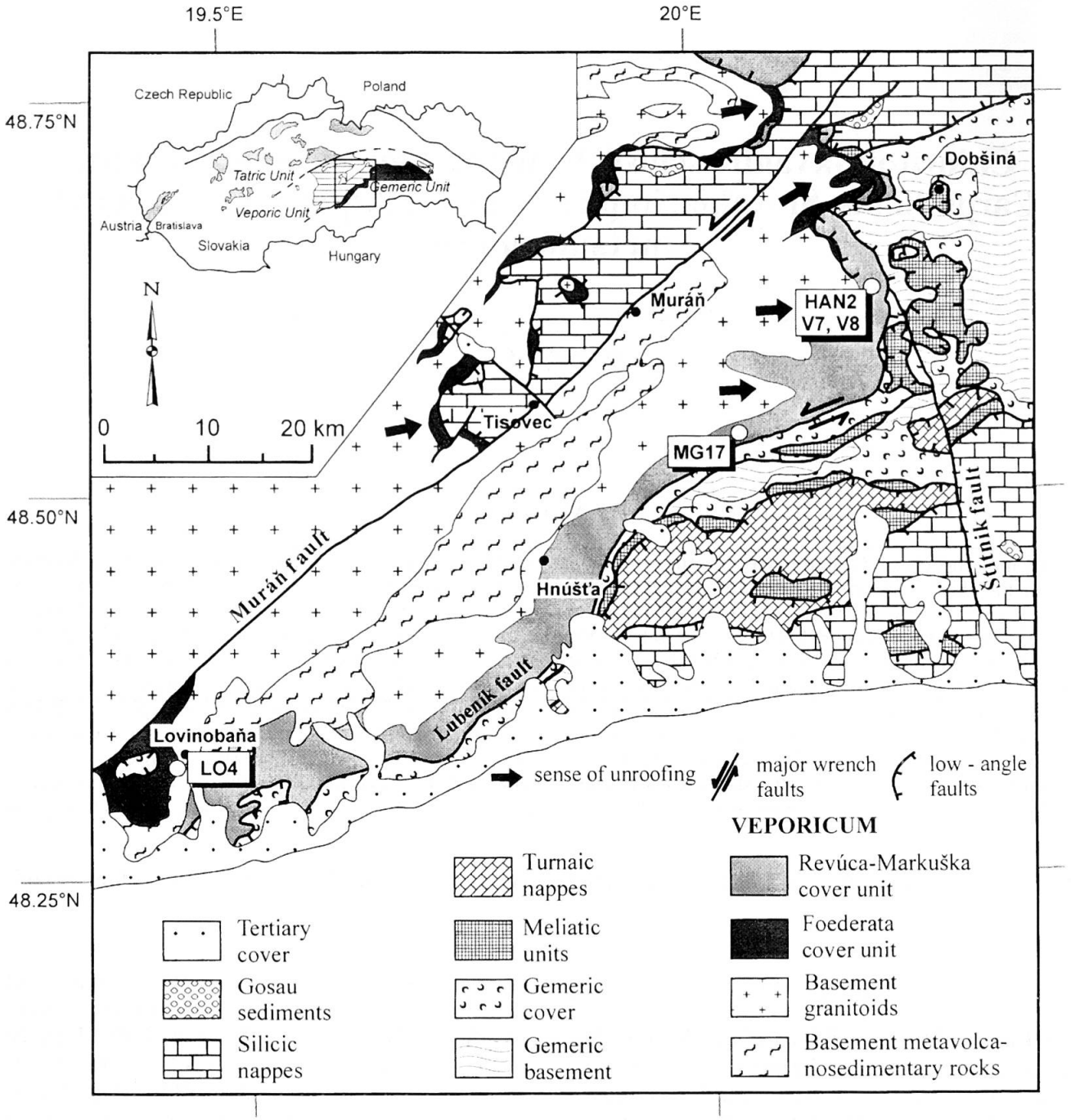

Fig. 1 Geological sketch map of the studied area with locations of investigated samples.

Alpine metamorphism was essentially interpreted to be low (e.g. CAMBEL and KORIKOVSKY, 1986; KRIST et al., 1992; BEZÁK et al., 1993).

In the Veporic unit, regional Alpine metamorphism of greenschist facies has been documented by several authors (e.g. VRÁNA, 1964; VOZÁROVÁ, 1990; BEZÁK, 1991; KOVÁČIK, 1996; KOVÁČIK et al., 1996; KORIKOVSKY et al., 1997). In contrast, MÉRES and HOVORKA (1991) and more recently PLAŠIENKA et al. (1999) and KOROKNAI et al. (1999) have emphasized that Alpine metamorphism reached even higher grade, up to middle amphibolite facies conditions (~ 600 °C; 10 kbar, PLAŠIENKA et al., 1999) in the staurolite and kyanite-bearing micaschists.

This study is focused on chloritoid and kyanite-bearing metapelites in the Permo-Triassic cover of the Veporic unit. These rocks were investigated by VRÁNA (1964), VOZÁROVÁ (1990) and KORIKOVSKY et al. (1989, 1997), however, no thermobarometric data have been reported until now. The purpose of this paper is to determine the P-T conditions from thermobarometry using internally consistent thermodynamic data (HOLLAND and POWELL, 1998) and an exchange Fe–Mg chloritoid-chlorite thermometer (VIDAL et al., 1999).

Compositional zoning of chloritoid and deformational microtextures are discussed with respect to tectonometamorphic evolution of the Veporic unit during Cretaceous orogeny.

Geological setting

The study area occurs in the south-eastern part of the Veporic unit exhibiting the topmost cover complexes along the contact with the overlying Gemeric unit (Fig. 1). This contact – the Lubeník line – was originally an overthrust fault and its straight SW–NE trending segment was reactivated as a sinistral transpressional zone, while the NW–SE sector was reactivated as a NE-dipping low-angle extensional normal fault (Fig. 1). The Veporic unit consists of several basement complexes assembled during the Variscan orogeny that are overlain by an Upper Palaeozoic–Triassic sedimentary cover. In the central and NE part of the Veporicum, the locally preserved cover includes Upper Permian sandstones and conglomerates, Scythian quartzites and slates and Middle–Upper Triassic carbonates and shales (Foederata unit). The SE rim is composed of Carboniferous and Permian (Revúca Group) and Scythian clastic sequences forming a partly allochthonous unit (Markuška nappe) overthrusting the Foederata cover unit to the NW. All these Veporic cover units were affected by Alpine regional metamorphism of low to medium grade (VRÁNA, 1964; PLAŠIENKA et al., 1989; KORIKOVSKY et al., 1997; LUPTÁK et al., 1999).

The deformational structures of the area are dominated by a flat or moderately NE to SE-dipping metamorphic/mylonitic foliation (S_1) that is penetrative in both the topmost parts of the basement granitoids and the Veporic cover units. The foliation planes bear a distinct stretching lineation (L_1) plunging generally to the east. These structures formed during the first deformation stage (AD_1), including moderately E- to NE-dipping shear bands which are mesoscopically penetrative in the neighbourhood of the NW–SE trending sector of the Lubeník line (extensional crenulation cleavage–ecc, or C'-type shear bands). Shear bands and other shear-sense criteria point to top-to-the-east kinematics. The growth of newly formed metamorphic minerals (micas, chloritoid, kyanite) within the cover rocks is generally syn- to early post-kinematic with respect to the foliation (S_1), and pre- to syn-kinematic with respect to the C' planes.

The (AD_1) structures represent a large-scale subhorizontal ductile shear zone. This shear zone is interpreted as a low-angle detachment fault zone that parallels the basement/cover interface and lithological boundaries within the Veporic cover, as well as the original Veporic/Gemeric overthrust contact (PLAŠIENKA, 1993; HÓK et al., 1993; MADARÁS et al., 1996). This detachment fault was active during the Late Cretaceous exhumation of the Veporic metamorphic core complex. Orogen-parallel extension was accompanied and followed by orogen-normal contraction producing superimposed deformation stages (PLAŠIENKA, 1993).

The timing of the principal Alpine deformation events in the Veporicum is constrained by $^{40}Ar/^{39}Ar$ isotopic data (MALUSKI et al., 1993; DALLMEYER et al., 1996; KOVÁČIK et al., 1996), recording cooling ages between ~ 110 and 80 Ma. Apatite fission tracks ages from granitoids point to Upper Cretaceous to Paleogene cooling (KRÁĽ, 1977). The extension and exhumation of the southern part of the Veporicum culminated by intrusion of the Rochovce granite 82 Ma ago (HRAŠKO et al., 1999). This intrusion caused contact metamorphism overprinting the regional metamorphic assemblages (KORIKOVSKY et al., 1986; VOZÁROVÁ, 1990).

Petrography and deformational microtextures

The investigated rocks are fine-grained, with well-developed S–C' fabric (Fig. 2). Primary and retrograde assemblages have been recognised with respect to deformation. The primary metamorphic assemblage chloritoid + kyanite + chlorite + quartz + white mica ± rutile ± tourmaline is oriented into the (S_1) foliation planes, resulting from the regional metamorphism and crustal thickening. The (S_1) foliation is defined by alignment of chloritoid and kyanite porphyroblasts, as well as white mica and quartz (Fig. 2a, b). Subsequent shearing has rotated and bent the foliation into the C'-planes (Fig. 2c), which is interpreted as a consequence of post-burial top to the NE extension and unroofing. Chloritoid is sometimes replaced along its margins by chlorite, but mostly it remains fresh. In some cases, chlorite is growing in the C'-planes together with white mica.

Three textural types of chloritoid porphyroblasts have been distinguished with respect to the S–C' fabric. In the first case (Fig. 2d), chloritoid porphyroblasts which grew parallel to the foliation are affected by shear along C' resulting in typical S-shaped porphyroblasts. In the second case (Fig. 2e), chloritoid porphyroblasts are oriented at a low angle to the (S_1) foliation. The foliation is truncated at the contact with chloritoid porphyroblasts. Chloritoid is sometimes rounded

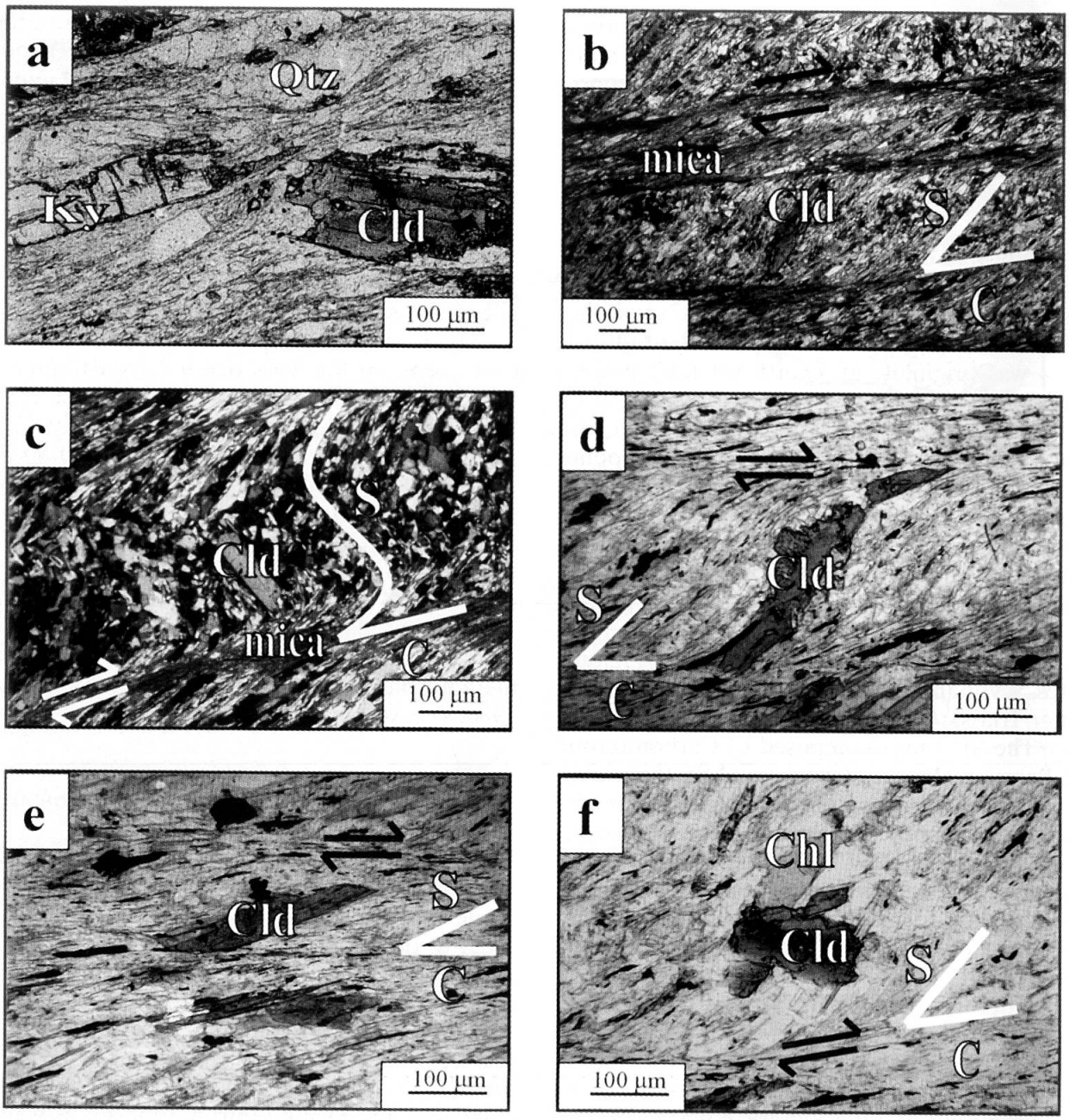

Fig. 2 Microphotographs of mineral assemblages and deformational textures in the chloritoid-kyanite schists from the Veporic unit. (a) Chloritoid and kyanite porphyroblasts. (b) Deformational S–C texture. (c) Bending of S planes into the shear bands C. (d, e and f) Three textural types of chloritoid porphyroblasts as described in the text.

at the ends of the crystals with respect to the principal compressive stress direction, which is interpreted as a pressure solution effect (PRIOR, 1987). In the third case (Fig. 2f), chloritoid porphyroblasts are present in thin quartz-rich microlithons, being oblique and/or oriented at a high angle with respect to the foliation. This microtextural type of chloritoid has a typical hourglass texture.

Analytical methods

Mineral identification and their chemical composition were evaluated by means of optical, X-ray powder diffraction and electron microprobe methods. The X-ray diffractograms of minerals from the whole-rock samples were obtained with a Philips PW 1710 diffractometer at the Geological Institute, Slovak Academy of Sciences in Bratislava. The operating conditions were CuKα radiation, 0.02 °2θ scan step size and 0.8 s scan step time, the tube current of 20 mA and generator voltage of 35 kV. In order to identify the phyllosilicates, the samples were separated into three fractions: < 2 μm, 2–6 μm and 6–20 μm by repeated settling in distilled water. These were analysed as oriented slides with a Siemens D-500 diffractometer at the Mineralogisch-Petrographisches Insti-

Tab. 1 Representative chemical analyses of chloritoid rims. Formulas calculated on the basis of 24 oxygens and 16 cations p.f.u.

Sample	HAN2	V 7	V 7	V8	V8	LO4a	MG17
analysis #	Cld10	Cld1	Cld13	Cld10	Cld14	Cld2	Cld5
SiO_2	24.71	24.21	24.24	24.45	24.76	24.89	24.07
TiO_2	0.03	0.15	0.00	0.00	0.00	0.04	0.00
Al_2O_3	40.67	41.46	41.14	40.58	41.51	42.00	40.24
FeO	21.88	22.25	22.52	22.21	20.40	22.19	22.06
MnO	0.47	0.45	0.37	0.29	0.31	0.38	1.05
MgO	4.40	4.39	4.13	4.17	4.67	3.92	3.67
CaO	0.00	0.02	0.01	0.00	0.00	0.00	0.00
Na_2O	0.00	0.00	0.00	0.00	0.00	0.01	0.02
K_2O	0.03	0.00	0.00	0.00	0.00	0.03	0.02
Total	92.19	92.93	92.41	91.70	91.65	93.46	91.13
Si	4.036	3.924	3.956	4.020	4.036	4.012	3.996
Ti	0.004	0.020	0.000	0.000	0.000	0.004	0.000
Al	7.832	7.920	7.916	7.864	7.980	7.984	7.876
Fe^{3+}	0.096	0.200	0.176	0.096	0.000	0.000	0.144
Fe^{2+}	2.892	2.816	2.900	2.956	2.780	2.992	2.920
Mn	0.064	0.060	0.052	0.040	0.044	0.052	0.148
Mg	1.072	1.060	1.004	1.024	1.136	0.940	0.908
Ca	0.000	0.004	0.000	0.000	0.000	0.000	0.000
Na	0.000	0.000	0.000	0.000	0.000	0.004	0.008
K	0.008	0.000	0.000	0.000	0.000	0.008	0.004
Fe/(Fe+Mg)	0.730	0.727	0.743	0.743	0.710	0.761	0.763

Tab. 2 Representative chemical analyses of chlorite. Formulas calculated on the basis of 28 oxygen atoms p.f.u., assuming all Fe as Fe^{2+}.

Sample	HAN2	V7	V7	V7	V8	V8	LO4a	LO4a
Analysis #	Chl11	Chl5	Chl12	Chl15	Chl9	Chl13	Chl1	Chl4
SiO_2	25.51	24.79	25.45	25.51	25.05	25.43	25.03	25.73
TiO_2	0.28	0.06	0.09	0.17	0.00	0.00	0.05	0.02
Al_2O_3	23.35	24.79	24.93	24.59	24.64	23.71	22.27	23.91
FeO	21.28	19.20	18.97	19.12	19.59	19.29	25.61	20.07
MnO	0.14	0.07	0.08	0.09	0.12	0.12	0.43	0.21
MgO	17.22	17.47	17.71	18.02	17.90	18.61	15.63	18.76
CaO	0.03	0.01	0.00	0.02	0.00	0.00	0.00	0.06
Na_2O	0.05	0.01	0.04	0.02	0.00	0.00	0.00	0.01
K_2O	0.04	0.02	0.01	0.03	0.00	0.00	0.00	0.00
Total	87.90	86.42	87.28	87.57	87.30	87.16	89.02	88.77
Si	5.236	5.115	5.183	5.186	5.126	5.206	5.207	5.192
Ti	0.043	0.009	0.014	0.026	0.000	0.000	0.008	0.003
Al	5.650	6.030	5.985	5.893	5.945	5.723	5.462	5.686
Fe^{2+}	3.653	3.314	3.231	3.251	3.352	3.303	4.456	3.387
Mn	0.024	0.012	0.014	0.015	0.020	0.020	0.076	0.036
Mg	5.267	5.373	5.375	5.459	5.460	5.679	4.846	5.642
Ca	0.007	0.002	0.000	0.004	0.000	0.000	0.000	0.013
Na	0.020	0.004	0.016	0.008	0.000	0.000	0.000	0.004
K	0.010	0.005	0.003	0.008	0.000	0.000	0.000	0.000
Fe/(Fe+Mg)	0.409	0.381	0.375	0.373	0.380	0.368	0.479	0.375

tut, University of Basel. The operating conditions were CuKα radiation, 0.02 °2θ scan step size and 1 s scan step time; the tube current was 40 mA and the generator voltage of 30 kV. Chemical analyses of selected minerals were performed by WDS method using the Jeol JXA-8600 electron-microprobe at the Mineralogisch-Petrographisches Institut, University of Basel. The operating conditions were set at 15 kV and 10 nA, natural and synthetic standards were used and the data were

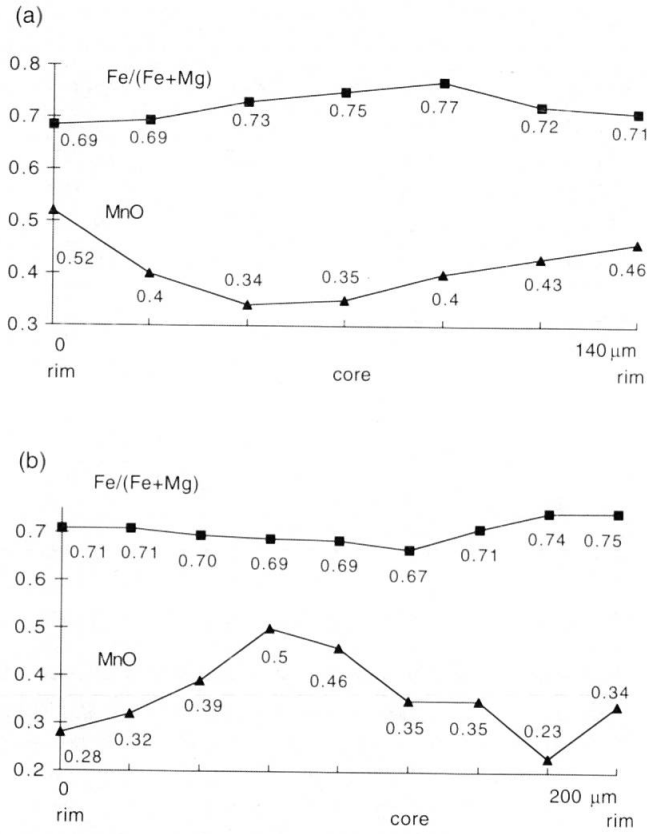

Fig. 3 Distribution of Fe/(Fe+Mg) and MnO across representative chloritoid porphyroblasts. (a) Prograde chloritoid zoning, sample V7. (b) Retrograde chloritoid zoning, sample HAN2.

reduced by PROZA routine. Mineral abbreviations are according to KRETZ (1983).

Mineral chemistry

CHLORITOID

Representative rim compositions of chloritoid porphyroblasts are reported in table 1. The Fe^{3+} content was calculated on the basis of 24 oxygens and 16 cations. The resulting values of Fe^{3+} in chloritoid are up to 0.200. Main chemical variations concern the divalent cations Fe^{2+}, Mn^{2+} and Mg^{2+}. The content of Mn^{2+} is mostly low. Most of the chloritoid porphyroblasts are compositionally zoned. Two types of zonation can be observed. Type A (Fig. 3a) is characterised by a gradual increase in $X_{Mg} = Mg/(Mg+Fe^{2+})$ from core to rim; X_{Mg} increasing from 0.17–0.28 (core) to 0.20–0.36 (rim). This type of chloritoid zoning is most common for samples showing textural equilibrium with chlorite, kyanite and rutile. On the other hand, the reverse pattern type B (Fig. 3b), with decreasing X_{Mg} from core (0.35–0.26) to rim (0.29–0.24) has been detected in chloritoids that are partially replaced by chlorite (Fig. 4). Consequently, type A is interpreted as prograde, whereas type B as retrograde zoning of chloritoid porphyroblasts due to Fe^{2+}-Mg cation exchange between chloritoid and chlorite (FRANCESCHELLI, 1997).

CHLORITE

Representative analyses of chlorite are shown in table 2. The analysed chlorites have a Fe/(Fe+Mg) ratio ranging from 0.37 to 0.48 and MnO is present up to 0.43 wt%. Compositional variability can be distinguished among texturally distinct chlorite types. Primary chlorite, in apparent textural equilibrium with chloritoid, is more magnesian (Fe/(Fe+Mg) ~ 0.37–0.40) than the one (Fe/(Fe+Mg) ~ 0.41–0.48) showing disequilibrium features, such as replacement of chloritoid or formation in late-stage veinlets in extensional cracks. This might be due to retrograde net-transfer reactions producing chlorite at the expense of a more Fe-rich phase, i.e. chloritoid.

WHITE MICA

Representative analyses of white mica are in table 3. Potassic white micas vary in composition from phengite (Si up to 6.5 atoms p.f.u.) to muscovite. The highest Ti-content is about 0.04 atoms p.f.u. In some samples paragonite is also present (X_{Na} 0.74–0.93). X-ray diffraction study and electron beam-scanning X-ray images show that these white micas are intergrown with chlorite (Fig. 4). In one sample, margarite flakes ($X_{Ca} = 0.43$) have been identified.

P-T estimates

It is inferred that chloritoid could have been formed by reactions: Chl + 4Prl = 5Cld + 2Qtz + $3H_2O$ or Ilm + Chl_1 + Qtz = Cld + Chl_2 + Rt + H_2O during prograde metamorphism of high-Al sedimentary protolith. The presence of kyanite and the absence of pyrophyllite in the investigated metapelites suggest that the upper thermal stability of pyrophyllite was overstepped and kyanite was formed by the reaction Prl = Ky + 3Qtz + H_2O. On the other hand, the absence of staurolite and garnet indicates that the upper boundary of chloritoid stability, i.e. the breakdown of chloritoid to garnet and staurolite in presence of quartz was not reached.

To determine more precisely the P-T conditions, equilibria relevant to observed mineral as-

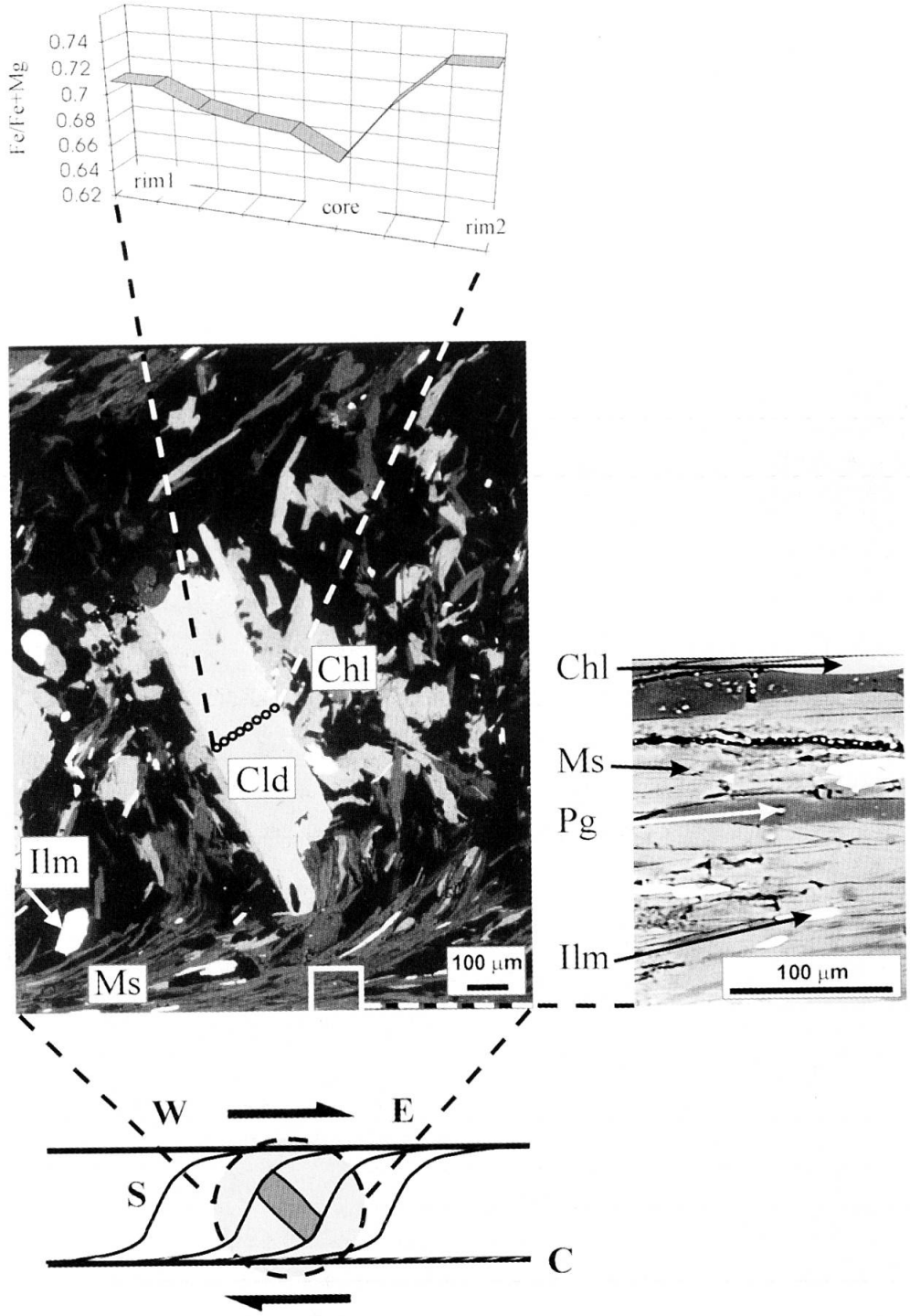

Fig. 4 Back-scattered electron image of chloritoid porphyroblast with retrograde zoning. Right side down; BSE image of phyllosilicates from shear planes C.

semblages were calculated using the computer program THERMOCALC v2.75 (POWELL and HOLLAND, 1988) and the internally consistent thermodynamic dataset of HOLLAND and POWELL (1998). The average P-T method approach (POWELL and HOLLAND, 1994) has been employed for the observed assemblages involving several linearly independent reactions in the K_2O–FeO–MgO–SiO_2–Al_2O_3–TiO_2–H_2O (KFMSATH) system. Mineral activities of chloritoid, chlorite and white mica (Tab. 4a) were calculated using the program AX included in the THERMOCALC v2.75 software. Activities of quartz, rutile, ilmenite and kyanite were taken to be unity. Fluid composition was assumed to be a simple binary H_2O–CO_2 mixture with variable X_{H2O} values (Tab. 4b). Mineral compositions were selected from domains of apparent textural equilibrium, i.e. chlorite in sharp contact with prograde-zoned chloritoid. Assuming that increasing X_{Mg} = Mg/

Tab. 3 Representative chemical analyses of white mica. Formulas calculated on the basis of 22 oxygen atoms p.f.u., all Fe as Fe^{2+}.

Sample	HAN2	HAN2	V7	V7	V8	V8	LO4	MG17
analysis #	Ms13	Pg20	Ms3	Ms13	Ms6	Ms13	Ms10	Mrg9
SiO_2	46.16	45.87	48.64	49.89	49.26	49.9	46.04	38.42
TiO_2	0.41	0.16	0.03	0.08	0.23	0.12	0.00	0.00
Al_2O_3	35.20	40.66	33.45	34.52	33.06	34.5	37.71	43.05
FeO	2.48	0.88	1.77	1.66	1.89	1.61	0.38	0.52
MnO	0.00	0.00	0.04	0.00	0.00	0.04	0.00	0.02
MgO	0.62	0.06	0.51	0.41	0.68	0.53	0.65	0.18
CaO	0.01	0.72	0.02	0.02	0.00	0.00	0.00	5.81
Na_2O	1.23	6.38	1.28	1.06	0.86	0.86	1.15	2.13
K_2O	9.10	1.07	9.22	9.10	9.17	8.59	8.98	3.14
Total	95.21	95.80	94.96	96.74	95.15	96.15	94.91	93.27
Si	6.148	5.855	6.445	6.468	6.505	6.478	6.069	5.154
Al^{iv}	1.852	2.145	1.555	1.532	1.495	1.522	1.931	2.846
Al^{vi}	3.675	3.974	3.682	3.740	3.652	3.758	3.929	3.963
Ti	0.041	0.015	0.003	0.005	0.023	0.012	0.000	0.000
Mg	0.123	0.011	0.101	0.079	0.134	0.103	0.128	0.036
Fe^{2+}	0.276	0.094	0.196	0.180	0.209	0.175	0.042	0.058
Mn	0.000	0.000	0.004	0.000	0.000	0.004	0.000	0.002
Ca	0.001	0.098	0.003	0.003	0.000	0.000	0.000	0.835
Na	0.318	1.579	0.329	0.266	0.220	0.216	0.294	0.554
K	1.546	0.174	1.560	1.505	1.545	1.423	1.510	0.538
Fe/(Fe+Mg)	0.692	0.895	0.660	0.695	0.609	0.629	0.247	0.617
X(Ca)	0.001	0.053	0.002	0.002	0.000	0.000	0.000	0.433
X(Na)	0.171	0.853	0.174	0.150	0.125	0.132	0.163	0.287
X(K)	0.829	0.094	0.825	0.848	0.875	0.868	0.837	0.279

Tab. 4a Mineral phases, end-member activities and their relative standard deviations sd(a)/a used in the THERMOCALC v2.75 calculations. End-member abbreviations after POWELL and HOLLAND (1988).

Sample		V7a		V7b		V8a		V8b		HAN2		LO4	
Mineral	End-M.	Activity	sd(a)/a	Activity	sd(a)/a	Activity	sd(a)/a	Activity	sd(a)/a	Activity	sd(a)/a	Activity	sd(a)/a
chloritoid		Cld1		Cld13		Cld10		Cld14		Cld10		Cld2	
	mctd	0.290	0.15	0.270	0.16	0.280	0.16	0.320	0.14	0.290	0.15	0.270	0.16
	fctd	0.690	0.05	0.710	0.05	0.730	0.05	0.720	0.05	0.710	0.05	0.076	0.05
chlorite		Chl5		Chl12		Chl9		Chl13		Chl11		Chl4	
	clin	0.071	0.32	0.072	0.32	0.071	0.32	0.080	0.31	0.054	0.35	0.074	0.32
	daph	0.007	0.59	0.006	0.60	0.007	0.59	0.006	0.60	0.010	1.04	0.007	0.60
	ames	0.068	0.33	0.075	0.32	0.071	0.32	0.077	0.31	0.056	0.35	0.075	0.32
muscovite		Ms3		Ms13		Ms6		Ms13		Ms13		Ms10	
	mu	0.670	0.10	0.680	0.10	0.660	0.10	0.660	0.10	0.660	0.10	0.760	0.10
	cel	0.016	0.46	0.013	0.47	0.016	0.63	0.016	0.45	0.014	0.71	0.008	0.50
quartz	q	1	0	1	0	1	0	1	0	1	0	1	0
rutile	ru	1	0	1	0	1	0	1	0	1	0	1	0
ilmenite	ilm	1	0	1	0	1	0	1	0	1	0	1	0
kyanite	ky	1	0	1	0	1	0	1	0	1	0	1	0

End-M.: End-Member.

($Mg+Fe^{2+}$) from core to rim in chloritoid is a prograde feature and associated chlorite is in equilibrium with the chloritoid rim, calculated P-T conditions may correspond to the peak of metamorphism.

The THERMOCALC results are summarised in Tab. 4b. Calculated temperature ranges from 500 to 590 °C and pressure from 4.5 to 7.7 kbar, at a presence of fluid with $X_{H2O} = 0.5–1.0$. Temperature calculated using the empirical chloritoid-chlorite Mg–Fe exchange thermometer of VIDAL et al. (1999) ranges between 480 and 580 °C (Tab. 5). For these temperatures, Vidal et al. (1992) re-

Tab. 4b Average P-T calculations using THERMOCALC v 2.75 (POWELL and HOLLAND, 1988) and thermodynamic data of HOLLAND and POWELL (1998).

Sample	V7a	V7a	V7a	V7b	V7b	V7b
$X_{(H2O)}$	1.0	0.7	0.5	1.0	0.7	0.5
T (°C)	588	560	542	573	547	529
s.d. (T)	33	30	30	39	36	35
P (kbar)	7.4	7.2	7.1	6.3	6.1	6.0
s.d. (P)	3.0	2.9	2.8	3.2	3.1	3.0
cor	0.949	0.944	0.937	0.959	0.955	0.949
f	1.53	1.54	1.55	1.69	1.69	1.70
N_R	5	5	5	5	5	5
Sample	V8a	V8a	V8a	V8b	V8b	V8b
$X_{(H2O)}$	1.0	0.7	0.5	1.0	0.7	0.5
T (°C)	574	547	529	586	558	541
s.d. (T)	43	40	39	35	32	32
P (kbar)	6.6	6.4	6.3	7.7	7.5	7.3
s.d. (P)	3.7	3.6	3.5	3.3	3.1	3.1
cor	0.968	0.965	0.960	0.945	0.940	0.932
f	1.67	1.67	1.67	1.69	1.70	1.71
N_R	5	5	5	5	5	5
Sample	LO4	LO4	LO4	HAN2	HAN2	HAN2
$X_{(H2O)}$	1.0	0.7	0.5	1.0	0.7	0.5
T (°C)	549	524	507	571	545	527
s.d. (T)	43	39	38	30	28	28
P (kbar)	4.7	4.6	4.5	6.4	6.2	6.1
s.d. (P)	3.1	2.9	2.8	2.5	2.5	2.5
cor	0.973	0.970	0.966	0.972	0.970	0.966
f	1.64	1.62	1.61	1.05	1.08	1.10
N_R	5	5	5	5	5	5

cor: correlation; f: fit parameter; N_R: number of independant reactions; s.d: standard deviation (POWELL and HOLLAND, 1988; 1994)

port pressure conditions between 5 and 8 kbar for the equilibrium Cld + Qtz = Chl + Ky, with X_{MgChl} ~ 0.62, X_{MgCld} = 0.26 – 0.3 and a_{H2O} = 1.

Taking into consideration the results of both thermobarometric methods and the upper stability limit of chloritoid (~ 550–560 °C at 5–8 kbar in KFMASH system) according to petrogenetic grid of SPEAR and CHENEY (1989), the P-T conditions of 530–560 °C and 6–8 kbar seem to be realistic for the peak of metamorphism in the investigated chloritoid-kyanite schists.

According to previous estimates, Alpine metamorphism in similar rocks from the SE Veporic unit reached 420–460 °C; 3–6 kbar (VOZÁROVÁ, 1990), 330–480 °C; 7–9 kbar (KORIKOVSKY et al., 1997) and 350–420 °C; 2.3–4 kbar in the metasomatic kyanite-Mg chlorite schists (KOVÁČIK, 1996).

Discussion

The presented data reveal that the investigated Veporic cover rocks experienced medium-temperature and medium-pressure collision-type metamorphism. The growth of peak metamorphic assemblages was syn- to partly post-kinematic with respect to the main metamorphic foliation (S_1) and pre-kinematic with respect to the macroscopically pervasive shear-band foliation C'. This shear-band foliation consistently indicates top-to-the-east shearing within a broad, low-angle, east-dipping, normal ductile shear zone affecting the Veporic cover complexes, the underlying basement granitoids, as well as the lowermost parts of the overlying Gemeric units along the eastern margin of the Veporic core. We interpret the flatly east-dipping shear zone as a detachment fault and the Lubeník Line as sinistral strike-slip, which both accommodated unroofing and exhumation of the Veporic complexes from below the tectonic overburden. According to the tectonic interpretation by PLAŠIENKA (1997), PLAŠIENKA et al. (1999), the overburden was formed by the Gemeric basement and cover units, the Meliatic subduction-collision complex and the Turnaic cover nappe system with the cumulative thickness of

Tab. 5 Temperatures calculated with the chloritoid-chlorite Mg–Fe exchange thermometer of VIDAL et al. (1999).

Sample	Chloritoid	Chlorite	cld X_{Fe2+}	cld X_{Mg}	chl X_{Fetot}	chl X_{Mg}	K_D	ln K_D	T (°C)
V7a	Cld1	Chl5	0.727	0.274	0.382	0.619	4.306	1.460	540
V7b	Cld13	Chl12	0.743	0.257	0.375	0.625	4.806	1.570	505
V8a	Cld10	Chl9	0.743	0.257	0.380	0.620	4.706	1.549	512
V8b	Cld14	Chl13	0.710	0.290	0.368	0.633	4.213	1.438	548
HAN2	Cld10	Chl11	0.730	0.270	0.409	0.591	3.892	1.359	576
LO4	Cld2	Chl4	0.761	0.239	0.375	0.625	5.304	1.668	476

~ 23–30 km (corresponding to the estimated pressure of 6–8 kbar). The north-vergent thrusting of these units preceded the metamorphic peak in the Veporicum by some tens of Ma and was probably related to the lower-plate crustal stacking due to continental collision after closure of the Meliata Ocean during the latest Jurassic – earliest Cretaceous (e.g. PLAŠIENKA et al., 1999). There are no reliable time constrains on timing of the metamorphic peak, but $^{40}Ar/^{39}Ar$ dating of white micas from the Veporic cover rocks presented by DALLMEYER et al. (1996) would indicate post-peak cooling and exhumation during the Late Cretaceous.

Summing up, our petrological and structural data suggest that the Veporic basement and cover complexes were first buried below a thick collision-related nappe stack, then they suffered medium-grade metamorphism and finally they were exhumed by an orogen-parallel extension during the Late Cretaceous.

Conclusions

The mineral assemblage chloritoid + chlorite + kyanite + phengite + rutile in the Permo-Triassic cover sequences of the Veporic unit, Central Western Carpathians, resulted from prograde metamorphism related to Cretaceous continental collision.

Chloritoid zoning, with increasing $X_{Mg} = Mg/(Mg+Fe^{2+})$ from core to rim reflects a prograde Fe^{2+}-Mg cation exchange between chloritoid and coexisting chlorite. A reverse pattern is interpreted as a consequence of retrogression.

Thermobarometric data suggest that metamorphic peak conditions reached 530–560 °C and 6–8 kbar, thus reflecting substantial crustal thickening due to the overburden formed by the Gemeric, Meliatic and Turnaic units.

The retrogression and transposition of mineral fabric into the C'-shear planes was due to top-to-the-E (orogen-parallel) extension that accomplished the exhumation and unroofing of the Veporic core complex along low-angle normal faults in Late Cretaceous time.

Acknowledgements

Research has been financially supported by the Swiss National Science Foundation (grant No 7SLPJ048664) and the Slovak Grant Agency for Science (project No 4075 and 7030) that is gratefully acknowledged. We thank O. Vidal and M. Kováčik for their constructive reviews, and M. Engi for his editorial help.

References

BEZÁK, V. (1991): Metamorphic conditions of the Veporic unit in the Western Carpathians. Geol. Carpath., 42, 219–222.

BEZÁK, V., SASSI, F.P., SPIŠIAK, J. and VOZÁROVÁ, A. (1993): An outline of the metamorphic events recorded in the Western Carpathians (Slovakia). Geol. Carpath., 44, 351–364.

BIELY, A. (1989): The geological structure of the West Carpathians. In: RAKÚS, M., DERCOURT, J. and NAIRN, A.E.M. (eds): Evolution of the northern margin of Tethys. Mém. Soc. Géol. France, Nouvelle Série No. 154 (II), Paris, 51–57.

CAMBEL, B. and KORIKOVSKY, S.P. (1986): Variscan retrograde metamorphism and Alpine diaphthoresis in the crystalline of the Western Carpathians. Geol. Zbor. Geol. Carpath., 39, 131–146.

DALLMEYER, R.D., NEUBAUER, F., HANDLER, R., FRITZ, H., MÜLLER, W., PANA, D. and PUTIŠ, M. (1996): Tectonothermal evolution of the internal Alps and Carpathians: Evidence from $^{40}Ar/^{39}Ar$ mineral and whole-rock data. Eclogae geol. Helv., 89, 203–227.

FRANCESCHELLI, M., MEMMI, I., CARCANGIU, G. and GIANELLI, G. (1997): Prograde and retrograde chloritoid zoning in low temperature metamorphism, Alpi Alpuane, Italy. Schweiz. Mineral. Petrogr. Mitt., 77, 41–50.

FRANK, W. (1987): Evolution of the Austroalpine elements in the Cretaceous. In: FLÜGEL, H. and FAUPL, P. (eds): Geodynamics of the Eastern Alps. Deuticke, Vienna, 379–406.

FREY, M., DESMONS, J. and NEUBAUER, F. (1999): The new metamorphic map of the Alps: Introduction. Schweiz. Mineral. Petrogr. Mitt., 79, 1–4.

HOINKES, G., KOLLER, F., RANITSCH, G., DACHS, E., HÖCK, V., NEUBAUER, F. and SCHUSTER, R. (1999): Alpine metamorphism of the Eastern Alps. Schweiz. Mineral. Petrogr. Mitt., 79, 155–181.

HÓK, J., KOVÁČ, P. and MADARÁS, J. (1993): Extensional tectonics of the western part of the contact area between the Veporicum and Gemericum (Western Carpathians). Mineralia Slov., 25, 172–176.

HOLLAND, T.J.B. and POWELL, R. (1998): An internally consistent thermodynamic data set for phases of petrological interest. J. Metamorphic Geol., 16, 309–343.

HRAŠKO, Ľ., HATÁR, J., HUHMA, H., MÄNTÄRI, I., MICHALKO, J. and VAASJOKI, M. (1999): U/Pb zircon dating of the Upper Cretaceous granite (Rochovce type) in the Western Carpathians. Krystalinikum, 25, 163–171.

KORIKOVSKY, S.P., JANÁK, M. and BORONIKHIN, V.A. (1986): Geothermometry and phase equilibria during recrystallization of garnet micachists to cordierite hornfelses in the aureole of Rochovce granite, Slovenské rudohorie Mts., area Rochovce-Chyžné. Geol. Zbor. Geol. Carpath., 37, 607–633.

KORIKOVSKY, S.P., KRIST, E. and BORONIKHIN, V.A. (1989): Staurolite-chloritoid schists from the Klenovec region: prograde metamorphism of high alumina rocks of the Kohút zone – Veporides. Geol. Zbor. Geol. Carpath., 39, 187–200.

KORIKOVSKY, S.P., PUTIŠ, M. and PLAŠIENKA, D. (1997): Cretaceous low-grade metamorphism of the Veporic and North-Gemeric Zones: a result of collisional tectonics in the central Western Carpathians. In: GRECULA, P., HOVORKA, D. and PUTIŠ, M. (eds): Geological Evolution of the Western Carpathians. Mineralia Slovaca-Monograph, Geocomplex, Bratislava, 107–130.

KOROKNAI, B., HORVÁTH, P., BALOGH, K. and DUNKL, I. (1999): Alpine metamorphic evolution and cooling history of the Veporic crystalline basement in Northern Hungary: new petrological and geochronological constraints. Tübinger Geowiss. Arbeiten, Series A, 52, 123–124.

KOVÁČIK, M. (1996): Kyanite-magnesian chlorite schist and its petrogenetic significance (the Sinec Massif, Southern Veporic Unit, Western Carpathians). Geol. Carpath., 47, 245 –255.

KOVÁČIK, M., KRÁĽ, J. and MALUSKI, H. (1996): Metamorphic rocks in the Southern Veporicum basement: their Alpine metamorphism and thermochronologic evolution. Mineralia Slov., 28, 185–202.

KRÁĽ, J. (1977): Fission track ages of apatites from some granitoid rocks in West Carpathians. Geol. Zbor. Geol. Carpath., 28, 269–276.

KRETZ, R. (1983): Symbols for rock-forming minerals. Am. Mineral., 68, 277–279.

KRIST, E., KORIKOVSKY, S.P., PUTIŠ, M., JANÁK, M. and FARYAD, S.W. (1992): Geology and petrology of metamorphic rocks of the Western Carpathian crystalline complexes. Comenius University Press, Bratislava, 324 pp.

LUPTÁK, B., FREY, M., JANÁK, M., SCHMIDT, S.TH. and PLAŠIENKA, D. (1999): Alpine metamorphism of the Mesozoic cover rocks from the Veporic unit, Western Carpathians: X-ray and EMP study of white mica and chlorite. Geol. Carpath., 50, 122–123.

MADARÁS, J., HÓK, J., SIMAN, P., BEZÁK, V., LEDRU, P. and LEXA, O. (1996): Extension tectonics and exhumation of crystalline basement of the Veporicum unit (Central Western Carpathians). Slovak Geol. Mag., 3–4, 179–183.

MALUSKI, H., RAJLICH, P. and MATTE, P. (1993): ^{40}Ar –^{39}Ar dating of the Inner Carpathians Variscan basement and Alpine mylonitic overprint. Tectonophysics, 223, 313–337.

MÉRES, Š. and HOVORKA, D. (1991): Geochemistry and metamorphic evolution of the Kohút crystalline complex mica schists (Western Carpathians). Acta Geol. Geograph. Univ. Comenianae, Geologica, 47, 15–66.

POWELL, R. and HOLLAND, T.J.B. (1988): An internally consistent thermodynamic dataset with uncertainties and correlations: 3. Application to geobarometry worked examples and a computer program. J. Metamorphic Geol. 6, 173–204.

POWELL, R. and HOLLAND, T.J.B. (1994): Optimal geothermometry and geobarometry. Am. Mineral., 79, 120–133.

PLAŠIENKA, D. (1993): Structural pattern and partitioning of deformation in the Veporic Foederata cover unit (Central Western Carpathians). In: RAKÚS, M. and VOZÁR, J. (eds): Geodynamic model and deep structure of the Western Carpathians. D. Štúr Inst. Geol., Bratislava, 269–277.

PLAŠIENKA, D. (1997): Cretaceous tectonochronology of the Central Western Carpathians, Slovakia. Geol. Carpath., 48, 99–111.

PLAŠIENKA, D., JANÁK, M., HACURA, A. and VRBATOVIČ, P. (1989): First illite crystallinity data from the Alpine metamorphosed rocks of the Veporicum. Miner. Slov., 21. 43–51.

PLAŠIENKA, D., GRECULA, P., PUTIŠ, M., HOVORKA, D. and KOVÁČ, M. (1997): Evolution and structure of the Western Carpathians: an overview. In: GRECULA, P., HOVORKA, D. and PUTIŠ, M. (eds): Geological Evolution of the Western Carpathians. Mineralia Slovaca-Monograph, Geocomplex, Bratislava, 107–130.

PLAŠIENKA, D., JANÁK, M., LUPTÁK, B., MILOVSKY, R. and FREY, M. (1999): Kinematics and metamorphism of a Cretaceous core complex: the Veporic unit of the Western Carpathians. Phys. Chem. Earth (A), 24, 651–658.

PRIOR, D.J. (1987): Syntectonic porphyroblast growth in phyllites: textures and processes. J. Metamorphic Geol., 5, 27–39.

PUTIŠ, M. (1991): Geology and petrotectonics of some shear zones in the West Carpathian crystalline complexes. Mineralia Slov., 23, 459–473.

SPEAR, F.S. and CHENEY, J.T. (1989): A petrogenetic grid for pelitic schists in the system SiO_2–Al_2O_3–FeO–MgO–K_2O–H_2O. Contrib. Mineral. Petrol., 101, 149–164.

THÖNI, M. and JAGOUTZ, E. (1992): Some new aspects of dating eclogites in orogenic belts: Sm–Nd, Rb–Sr and Pb–Pb isotopic results from the Austroalpine Saualpe and Koralpe type-locality (Carinthia/Styria, SE Austria). Geochim. Cosmochim. Acta. 56, 347–368.

TOMEK, Č. (1993): Deep crustal structure beneath the central and inner West Carpathians. Tectonophysics, 226, 417–431.

VIDAL, O., GOFFÉ, B., BOUSQUET, R. and PARRA, T. (1999): Calibration and testing of an empirical chloritoid-chlorite Mg–Fe exchange thermometer and thermodynamic data for daphnite. J. Metamorphic Geol., 17, 25–39.

VIDAL, O., GOFFÉ, B. and THEYE, T. (1992): experimental study of the stability of sudoite and magnesiocarpholite and calculation of a new petrogenetic grid for the system FeO–MgO–Al_2O_3–SiO_2–H_2O. J. Metamorphic Geol., 10, 603–614.

VOZÁROVÁ, A. (1990): Development of metamorphism in the Gemeric/Veporic contact zone (Western Carpathians). Geol. Zbor. Geol. Carpath., 41, 475–502.

VRÁNA, S. (1964): Chloritoid and kyanite zone of Alpine metamorphism on the boundary of the Gemerides and the Veporides. (Slovakia). Krystalinikum, 2, 125–143.

Manuscript received January 5, 2000; revision accepted June 8, 2000.